Hindawi
Mathematical Problems in Engineering
Volume 2019, Article ID 7973591, 8 pages
https://doi.org/10.1155/2019/7973591

Research Article

Model Predictive Control of Electric Spring for Voltage Regulation and Harmonics Suppression

Yun Zou,[1] **Yinlong Hu**,[2] **and Sifan Cao**[3]

[1]*School of Automation, Nanjing University of Science and Technology, Nanjing 210094, China*
[2]*College of Energy and Electrical Engineering, Hohai University, Nanjing 210098, China*
[3]*School of Automation Engineering, University of Electronic Science and Technology of China, Chengdu 611731, China*

Correspondence should be addressed to Yun Zou; z_ouyun@163.com

Received 21 February 2019; Accepted 14 March 2019; Published 7 April 2019

Guest Editor: Qing Hui

This paper presents a model predictive control (MPC) strategy for electric spring (ES) to address the power quality problems, especially voltage regulation and harmonic suppression, which are more acute for a growing proportion of renewable energy generation to the grid. A Kalman filter is used to estimate the random variation of the supply voltage and extract the fundamental and harmonic components of the supply voltage, respectively. In this way, the supply voltage, which is treated as an external disturbance for the plant, can be established in the state-space model form. Such processing brings great convenience to the application of MPC and also lays a foundation for MPC to achieve an ideal control effect. Based on an integrated state-space model of the supply voltage and the ES, an MPC controller is designed for power quality improvement. Simulation studies are carried out and the simulation results are presented to verify the effectiveness and accuracy of the control strategy.

1. Introduction

Due to environmental pollution and excessive consumption of fossil energy, more and more attention has been paid to the research, development and utilization of renewable energy sources (RESs) [1]. The increasing proportion of renewable energy generation to the grid means that the inertia of the power system declines, which makes the demand side [2, 3] of the power system sensitive to voltage and frequency fluctuations. Nowadays, solar [4, 5] and wind power [6] are the two most common sources of renewable energy for grid-connected generation. However, their own limitations, mainly randomness and unpredictability [7], cause a variation of active and reactive power at the power generation side, which is expected to cause power system [8, 9] instability. In addition, it should also be considered that the harmonic distortion of line voltage is further aggravated by the additional power electronics used for renewable energy generation. As a consequence, the problems of power quality will be more and more serious with the increase of the proportion of renewable energy power generation, especially voltage fluctuation and harmonic distortion. These power quality problems will be a great concern for users.

Electric spring (ES) was first introduced in 2012 as a new smart grid technology to balance the power between the power supply and demand automatically [10]. Therefore, power mismatch between the generation side and the demand side can be effectively alleviated. So far, a significant amount of research work has been conducted and rich research results have been achieved, which mainly consist of basic analyses, topological structures, and control strategies of ESs. The most basic function of ESs to keep active and reactive power balance for mitigating voltage and frequency fluctuation is described in [11]. Dynamic modeling for ESs to implement large-scale simulation research and a general analysis on the steady-state behavior of ESs are introduced in [12] and [13, 14], respectively. The actual circuit and algorithm implementation of an ES to regulate the AC mains voltage by reactive power compensation is described in [15]. To reduce the use of energy storage equipment in the future smart grid with substantial renewable energy sources can be realized by ESs [16]. Voltage regulation in a microgrid by multiple

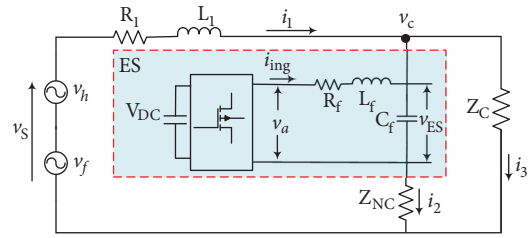

Figure 1: Overall simplified schematic diagram of the power system with an ES.

electric springs based on the distributed control is presented in [17], which can reduce the cost of centralized control [18] and compensate the inaccuracy of the traditional droop control effectively. In addition, there are also some research results about the use of ESs to improve power quality [19]. Harmonics suppression for the AC mains voltage by ESs with current-source inverters is introduced in [20]. However, in view of the above results, the research results about control strategies and control methods for ESs are relatively few, which mainly consists of the PI controller and the PR controller. The novel control strategy named δ control for ESs to provide different types of power/voltage compensations is presented in [21], which is significantly different from phase-locked control. A fuzzy logic controller designed for ESs to adjust the AC mains voltage is described in [22], which does not take into account the harmonics.

In this paper, model predictive control (MPC) [23–25] is combined with a Kalman filter [26] to be applied to ESs for harmonics suppression and voltage regulation for the first time, where the Kalman filter is used to estimate the random variation of the voltage source and to extract the fundamental and harmonic components, respectively. MPC is an online optimization control method based on a process prediction model, which comprehensively considers system constraints, dynamic responses, and control objectives. It should be noted that the online optimization problem of MPC is usually to solve a quadratic programming problem. The state-space model of ES presented in Section 3 is linear and time-invariant, which is greatly consistent with the requirement of online optimization of MPC. Furthermore, the most prominent advantage of model predictive control is the handling of hard constraints. For ES, the output voltage is realized by a Pulse Width Modulation (PWM) technology and its control signal is limited to ± 1. Thus, the active filter is guaranteed to operate in the linear modulation range.

The rest of this paper is organized as follows. In Section 2, the operating principle of ES for the smart grid with high penetration of renewable energy is described. The state-space model of ES is presented in Section 3. Section 4 describes the controller design based on MPC in detail. Numerical simulations are presented in Section 5 to verify the effectiveness of the control strategy. Section 6 draws the conclusions.

2. Basic Principles of Electric Spring

A simplified schematic diagram of a power system with an ES is shown in Figure 1. As distributed generation (e.g., such as wind and solar power generation) requires a large number of power electronic devices, the introduction of power harmonics is inevitable. With more and more distributed power supplies introduced to the power distribution network, the problem of harmonics will be more serious. Therefore, the supply voltage v_s can be represented by the sum of v_f (fundamental component) and v_h (harmonics component) in Figure 1. R_1 and L_1 are the equivalent resistance and inductance of the transmission line, respectively. The voltage at the point of common coupling (PCC) is represented by v_c, which is also the voltage across the critical load Z_c. It should be pointed out that Z_c represents a class of impedance that is sensitive to voltage fluctuation, while noncritical load Z_{nc} represents a class of impedance that can withstand a wide range of voltage fluctuations. Due to the characteristic of the noncritical load mentioned above, it withstands most of the power fluctuations of the grid. i_2 and i_3 are the currents flowing through the noncritical load Z_{nc} and critical load Z_c, respectively. i_1 is the line current. The ES in the red dotted box shown in Figure 1 includes a DC link capacitor, a PWM inverter [27, 28], and an LC filter. The voltage across the capacitor C_f is the output voltage of the ES, namely, V_{ES}. R_f is the equivalent resistance of the inverter transmission line. v_a is the output equivalent voltage of the PWM inverter. In the case of a half-bridge,

$$v_a = \frac{V_{DC}}{2} * u, \tag{1}$$

where V_{DC} is the DC link voltage, u is the modulation index [12] and also the output signal of the controller.

The ES was first proposed as a special reactive power compensator to regulate the line voltage v_c at its rated value with a standard sine wave at 50Hz in spite of v_s fluctuations. It injects a voltage, namely, v_{ES}, leading (or lags) the current flowing through the noncritical load for voltage suppression (or voltage boosting). In simple terms, ES mainly has two compensation modes, namely, inductive mode and capacitive mode to adjust the line voltage. When the voltage v_c exceeds its reference v_{c-ref}, v_{ES} leads i_0 by 90 degrees in the inductive mode for voltage suppression as shown in Figure 2, where v_0 and i_0 are the voltage and current of the noncritical load, respectively. When the voltage v_c under its reference v_{c-ref}, ES operates in the capacitive mode to boost the line voltage. It is noteworthy that the phase angle of v_c has a significant change before and after ES becomes effective as shown in Figure 2, which corresponds to v_s [21]. The internal phase relation between v_s and v_c is of great importance to the control design

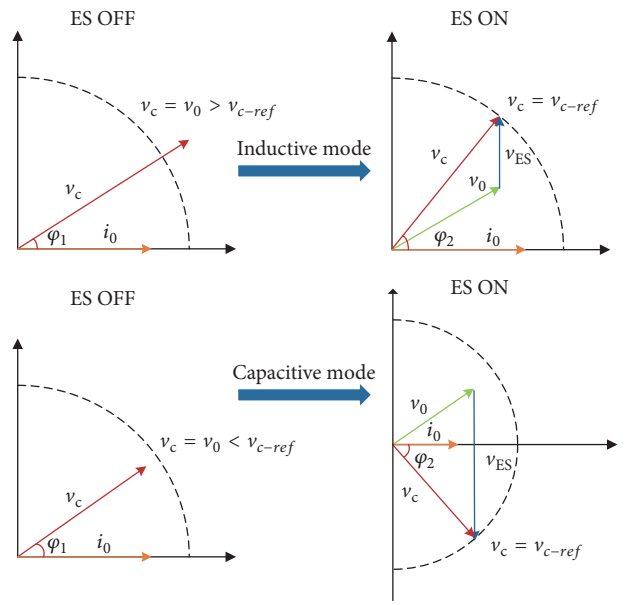

FIGURE 2: Operating modes of ES to adjust line voltage for a resistive-inductive load as a noncritical load (inductive mode for voltage suppression and capacitive mode for voltage boosting).

in Section 4, which determines the compensation mode of the ES. Once the DC link capacitor on the DC side of the inverter is replaced by an energy storage system, ES will not be limited to the above two modes of compensation [13].

3. Modelling of Electric Spring

The simplified power circuit of the ES with a supply voltage and transmission lines is shown in Figure 1. Applying Kirchhoff's Voltage and Current Laws, one obtains

$$L_1 \frac{di_1}{dt} = v_s - v_c - R_1 * i_1, \tag{2}$$

$$L_f \frac{di_{ing}}{dt} = v_a - v_{ES} - R_f * i_{ing}, \tag{3}$$

$$C_f \frac{dv_{ES}}{dt} = i_{ing} + i_2, \tag{4}$$

$$i_1 = i_2 + i_3, \tag{5}$$

$$i_2 = \frac{v_c - v_{ES}}{z_{NC}}, \tag{6}$$

$$i_3 = \frac{v_c}{z_C}. \tag{7}$$

Solving (1)–(7), a state-space model for the ES can be derived as

$$\dot{x} = A_e x + B_1 v_s + B_2 u, \tag{8}$$

$$y = C_e x + D_1 v_s + D_2 u, \tag{9}$$

where

$$A_e = \begin{bmatrix} -\dfrac{z_{NC}z_C + R_1(z_{NC}+z_C)}{L_1(z_{NC}+z_C)} & 0 & -\dfrac{z_C}{L_1(z_{NC}+z_C)} \\ 0 & -\dfrac{R_f}{L_f} & -\dfrac{1}{L_f} \\ \dfrac{z_{NC}}{C_f(z_{NC}+z_C)} & \dfrac{1}{C_f} & -\dfrac{1}{C_f(z_{NC}+z_C)} \end{bmatrix},$$

$$B_1 = \begin{bmatrix} \dfrac{1}{L_1} \\ 0 \\ 0 \end{bmatrix}, \tag{10}$$

$$B_2 = \begin{bmatrix} 0 \\ \dfrac{V_{DC}}{2L_f} \\ 0 \end{bmatrix},$$

$$C_e = \begin{bmatrix} \dfrac{z_{NC}z_C}{z_{NC}+z_C} & 0 & \dfrac{z_C}{z_{NC}+z_C} \end{bmatrix},$$

$$D_1 = 0,$$

$$D_2 = 0.$$

Denote the state vector as $x = [i_1 \;\; i_{ing} \;\; v_{ES}]^T$. Ideally, our control aim is to keep the line voltage v_c at its reference level all the time. Therefore, v_c, the core of our concern, should be considered as an output of the plant in the above state-space model. In addition, supply voltage v_s is treated as an external disturbance. u is the modulation index and also the control signal generated by the MPC controller, which is limited to ± 1. It is worth mentioning that the state-space model of ES is a multiple-input-single-output system with only one control input, which means that the complexity of control is greatly reduced. Note that the dynamic of V_{DC} is not considered for simplicity.

4. Control Design for Electric Spring

ES generates the compensation voltage v_{ES} through the PWM inverter technology based on the control signal u generated by the MPC controller to correct the harmonic distortion and adjust v_c to an ideal sine wave with an amplitude of 220 volts and a frequency of 50Hz under the condition that the supply voltage v_s fluctuates with time. In other words, our aim here is to regulate the line voltage v_c while suppressing the harmonics of v_c.

4.1. Disturbance Modeling. For the established state-space model of ES, the supply voltage v_s can be treated as a disturbance signal, which is fortunately a periodic and measurable signal. Thus, an exogenous model for v_s is employed to access the useful information immediately rather than after one

full period. The exogenous model is designed based on the following observation:

$$\frac{d}{dt}\begin{bmatrix}\cos(\omega_i t)\\ \sin(\omega_i t)\end{bmatrix} = \begin{bmatrix}0 & -\omega_i\\ \omega_i & 0\end{bmatrix}\begin{bmatrix}\cos(\omega_i t)\\ \sin(\omega_i t)\end{bmatrix}. \tag{11}$$

In this way, the periodic signal v_s, which consists of a finite number of harmonics, can be represented as

$$\dot{\xi} = A_\xi \xi, \tag{12}$$

$$v_s = C_\xi \xi, \tag{13}$$

where

$$\xi = \left[\cos(\omega_1 t), \sin(\omega_1 t), \cos(\omega_3 t), \sin(\omega_3 t), \cdots\right]^T, \tag{14}$$

and A_ξ is a block-diagonal matrix with the blocks given by

$$\begin{bmatrix}0 & -\omega_i\\ \omega_i & 0\end{bmatrix},$$
$$C_\xi = [1, 0, 1, 0, \cdots]. \tag{15}$$

In this way, the measured voltage v_s can be expressed in the form of state-space, which can be combined with the state-space model of ES to form a complete state-space model used for the MPC controller as follows:

$$\dot{\hat{x}} = A\hat{x} + Bu, \tag{16}$$

$$y = C\hat{x}, \tag{17}$$

where

$$A = \begin{bmatrix}A_e & B_1 C_\xi\\ 0 & A_\xi\end{bmatrix},$$
$$B = \begin{bmatrix}B_2\\ 0\end{bmatrix}, \tag{18}$$
$$C = [C_e \;\; 0].$$

Denote the state vector as $\hat{x} = [x \;\; \xi]^T$. Note that 0 in matrix A, matrix B, and matrix C is a vector, not a scalar, whose dimension depends on state ξ. That is to say, it has to do with the number of harmonics that we predefined. A Kalman filter [29] is used to estimate the state ξ from the measured voltage signal v_s by voltage sensors; thus the disturbance to the plant as mentioned in the previous section becomes ξ instead of v_s.

4.2. MPC Controller. The MPC controller designed for ES is based on the state-space model, while it cannot be applied to ES model (16)–(17) directly for the reason that MPC controller should apply to a discrete-time model. Therefore, model (16)–(17) should be discretized as follows:

$$\hat{x}(k+1) = A_d x + B_d u, \tag{19}$$

$$y(k) = C_d \hat{x}(k), \tag{20}$$

where A_d, B_d, C_d are the discrete forms of A, B, C in (16)–(17), respectively [29]. The method to construct the optimization problem in MPC is to expand the expression in the model to predict the state $\hat{x}$ and output v_c and then formulate a quadratic programming problem according to the control objective as follows:

$$J = \sum_{i=0}^{N_p-1} e(i)^T Q e(i) + \sum_{i=0}^{N_u-1} u(i)^T R u(i), \tag{21}$$

$$e(k) = y(k) - v_{c-ref}(k), \tag{22}$$

where Q, R are the positive definite gain matrices and N_u, N_p are the control horizon and the prediction horizon, respectively. In MPC, one should find u to minimize J and the first value of the control sequence u will be applied to the actuator; then the previous steps will be repeated at the next sampling time. It is noteworthy that the prominent feature of the MPC control strategy used in this paper is that the future characteristics of disturbance are fully taken into account in the online optimization based on the disturbance v_s modeling and the Kalman filter, which is an effective method for state estimation and prediction [26]. In fact, similar methods of Kalman filtering have been used to estimate harmonics in previous studies on power quality problems [30]. Specifically, the system model of the Kalman filter for the state estimation of v_s is defined as follows:

$$\xi_{i|i-1} = A_{\xi d}\xi_{i-1|i-1}, \tag{23}$$

$$P_{i|i-1} = A_{\xi d}P_{i-1|i-1}A_{\xi d}^T + Q, \tag{24}$$

$$K_{gi} = P_{i|i-1}C_\xi^T\left(C_\xi P_{i|i-1}C_\xi^T + R\right), \tag{25}$$

$$\xi_{i|i} = \xi_{i|i-1} + K_g\left(v_{s-m} - C_\xi \xi_{i|i-1}\right), \tag{26}$$

$$P_{i|i} = \left(I - K_{gi}C_\xi\right)P_{i|i-1}, \tag{27}$$

where $A_{\xi d}$ is the discrete form of A_ξ in (12), which is a block-diagonal matrix with each block taking $\begin{bmatrix}\cos(n\omega T_s) & -\sin(n\omega T_s)\\ \sin(n\omega T_s) & \cos(n\omega T_s)\end{bmatrix}$, T_s is the sampling time, and ω is the angular frequency of the grid. Q and R are the covariance matrices of the system noise and the measurement noise, respectively. P and K_g are the covariance matrix of the estimation error and the Kalman gain, respectively. $\xi_{i|i}$ is the estimation of ξ_i, while $\xi_{i|i-1}$ is the estimation at time instant $i-1$. v_{s-m} is the measurement of voltage v_s, which includes measurement noise. In this paper, the voltage v_s is treated as a measurable disturbance, so the Kalman filter can accurately estimate its state. It should be pointed out that the measurement noise R in the simulation is far less than the system noise Q because the random variation of v_s has a large deviation from the trajectory of the disturbance model. The overall control of the system based on the MPC controller with a Kalman filter [29] is shown in Figure 3. The supply voltage v_s is measured by the voltage sensors and transmitted to the Kalman filter to obtain the state ξ, which contains fundamental and harmonic components information. It should be pointed out that the selection of the phase of the reference voltage v_{c-ref} is closely

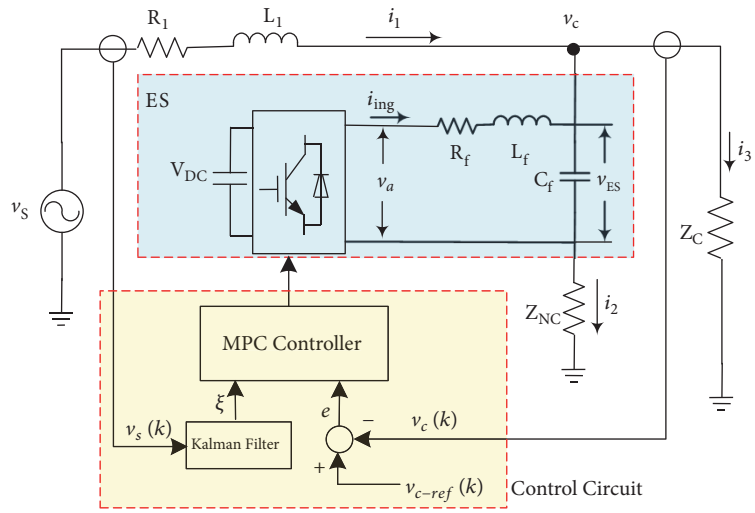

Figure 3: Control system block diagram of MPC-controlled ES with a Kalman filter.

Table 1: Simulated test system parameters.

Item	Value
Line resistance R_1	0.71 Ω
Line inductance L_1	19.92 mH
Critical load z_c	53 Ω
Non-critical load z_{nc}	50.5 Ω
Predefined reference value V_{c-ref}	220 V
DC voltage source V_{DC}	1200 V
Control horizon N_u	30
Prediction horizon N_p	30
System sampling time T_s	0.2 ms

related to the compensation modes of ES. Choosing different angles of v_{c-ref} can realize different functions of ES, such as power factor correction, constant reactive power compensation, constant real power compensation, and output voltage minimization of the ES.

5. Simulation Studies

To demonstrate the effectiveness of the control scheme proposed in this paper, four case studies are conducted by using MATLAB/SIMULINK. The Simulation parameters are shown in Table 1. Without loss of generality, the RMS of v_{c-ref} is assumed to be 220 V. The number of harmonics is up to the 15^{th}, which is used to simulate supply voltage harmonics.

5.1. Voltage Support Mode. In order to verify the voltage support capability of an ES under the MPC control strategy proposed in Section 4, supply voltage v_s is set below the rated value, which is used to simulate the situation of insufficient power output at the generation side. From Figure 4(a), one can observe a significant variation in the line voltage, namely, the voltage across critical loads, before and after the ES is activated. Before the ES is activated, the line voltage v_c is about 203 V, and it rises to the rated value (i.e., 220V) rapidly after the ES is activated at 1 second. Figures 4(b) and 4(c) show the corresponding output voltage of ES and control signal u, respectively.

5.2. Voltage Suppression Mode. To test the voltage suppression capability of an ES under the MPC control strategy, supply voltage v_s is set over the rated value, which is used to simulate the situation of excess power output on the generation side. From Figure 5(a), one can also observe a significant variation in the line voltage v_c before and after the ES is activated. Before ES is activated, the line voltage v_c is about 228 V, and it drops to the rated value (i.e., 220V) rapidly after the ES is activated at 1 second. Figures 5(b) and 5(c) show the corresponding output voltage of ES and control signal u, respectively.

5.3. Harmonic Compensation for Line Voltage. In order to illustrate the ability of an ES to regulate the voltage while suppressing voltage harmonics at the same time under the proposed MPC control strategy, supply voltage v_s is set below the rated value, and up to the 15^{th} order of the odd harmonics are added to v_s, which is closer to the real voltage with an increasing proportion of renewable energy fed into the power grid. As clearly seen from Figure 6(a), the line voltage v_c is not only smaller than the rated value, but the waveform is non-smooth with a large harmonic distortion before the ES is activated. After the ES is activated at 1 second, the waveform of the line voltage v_c is effectively improved, whose total harmonics distortion (THD) value is reduced from 18.79% to 1.36% as shown in Figures 6(b) and 6(c). Therefore, an ES with the MPC controller can deal with voltage regulation and harmonic correction satisfactorily.

5.4. Random Variations in Supply Voltage. To further verify the ability of an ES with the MPC controller for voltage regulation and waveform correction under extreme conditions, the supply voltage is set from step change to rapid

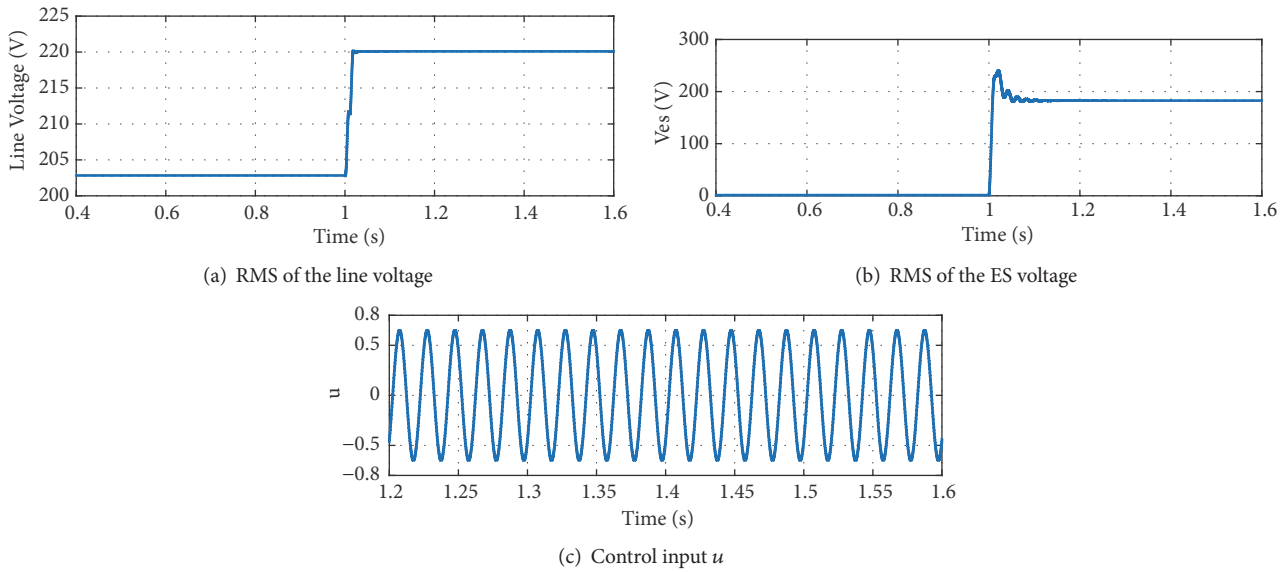

(a) RMS of the line voltage

(b) RMS of the ES voltage

(c) Control input u

FIGURE 4: Comparison of the changes before and after the ES is activated for voltage boosting. (a) RMS of the line voltage, (b) RMS of the ES voltage, and (c) control input u.

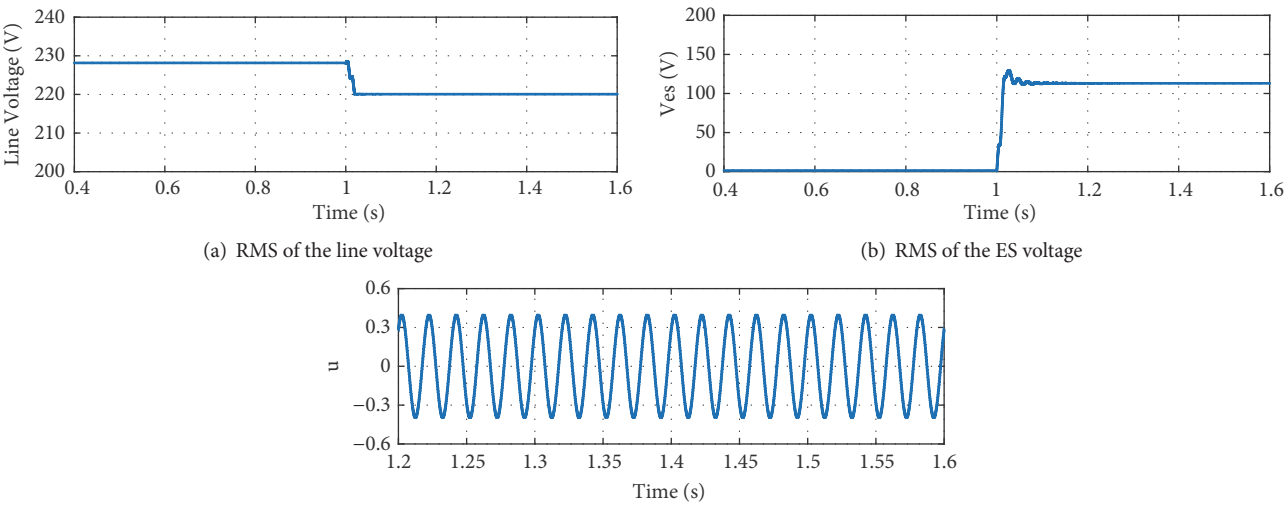

(a) RMS of the line voltage

(b) RMS of the ES voltage

(c) Control input u

FIGURE 5: Comparison of the changes before and after the ES is activated for voltage suppression. (a) RMS of the line voltage, (b) RMS of the ES voltage, and (c) control input u.

random change accompanied by relatively large fluctuations. However, the line voltage v_c is tightly regulated at 220V as shown in Figure 7(a). If one zooms in and looks at the waveform of v_c as shown in Figure 7(b), one can see that the waveform of v_c is corrected greatly, which shows that the ES is powerful enough to be used for voltage regulation and harmonics suppression. Figure 7(c) shows the corresponding output voltage of the ES.

6. Conclusion

This paper presented a new control strategy based on MPC for ESs to improve the power quality, mainly about voltage regulation and harmonic suppression. A Kalman filter was used to estimate the random variation of the supply voltage and extract the fundamental and harmonic components of the supply voltage, respectively. In this way, the supply voltage, which was treated as an external disturbance for the plant, could be incorporated in the state-space model form. Then, the supply voltage model was integrated with the ES model into a complete state-space model used for the model predictive controller design. The effectiveness and accuracy of using an ES under the MPC control strategy were verified by the simulation studies, which showed that MPC controller has the capability of realizing voltage regulation and restraining harmonics effectively at the same time.

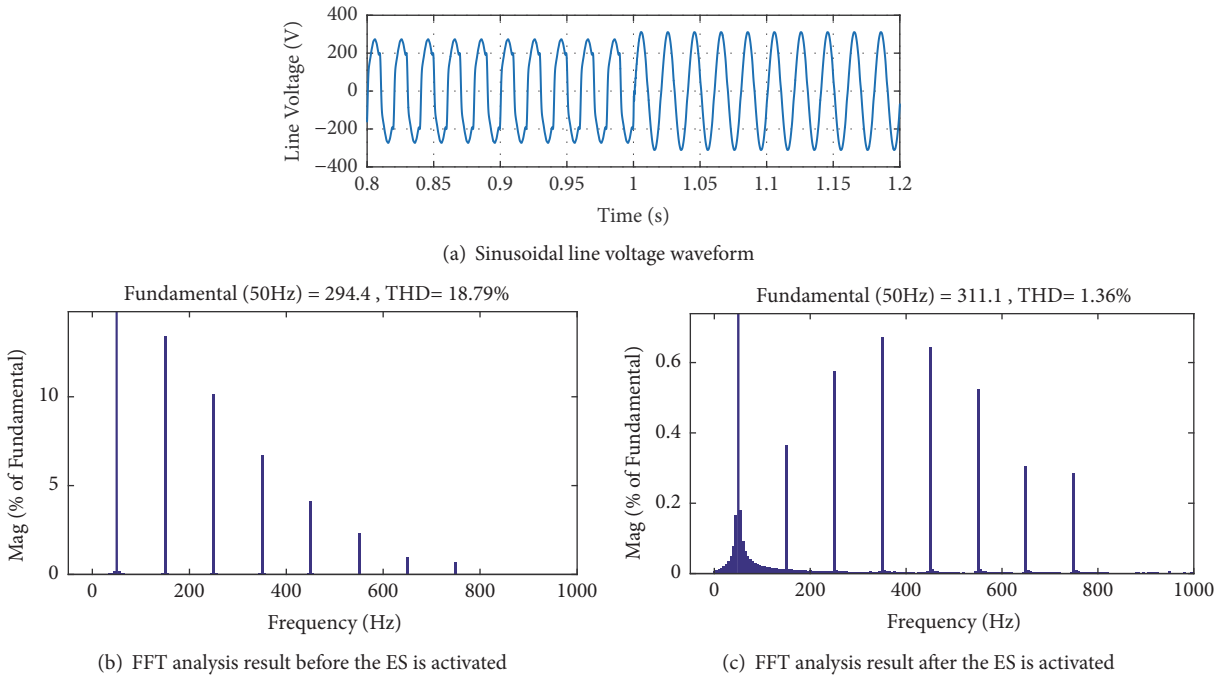

(a) Sinusoidal line voltage waveform

(b) FFT analysis result before the ES is activated

(c) FFT analysis result after the ES is activated

Figure 6: Sinusoidal line voltage waveform and results of the FFT analysis before and after the ES is activated. (a) Sinusoidal line voltage waveform, (b) FFT analysis result before the ES is activated, and (c) FFT analysis result after the ES is activated.

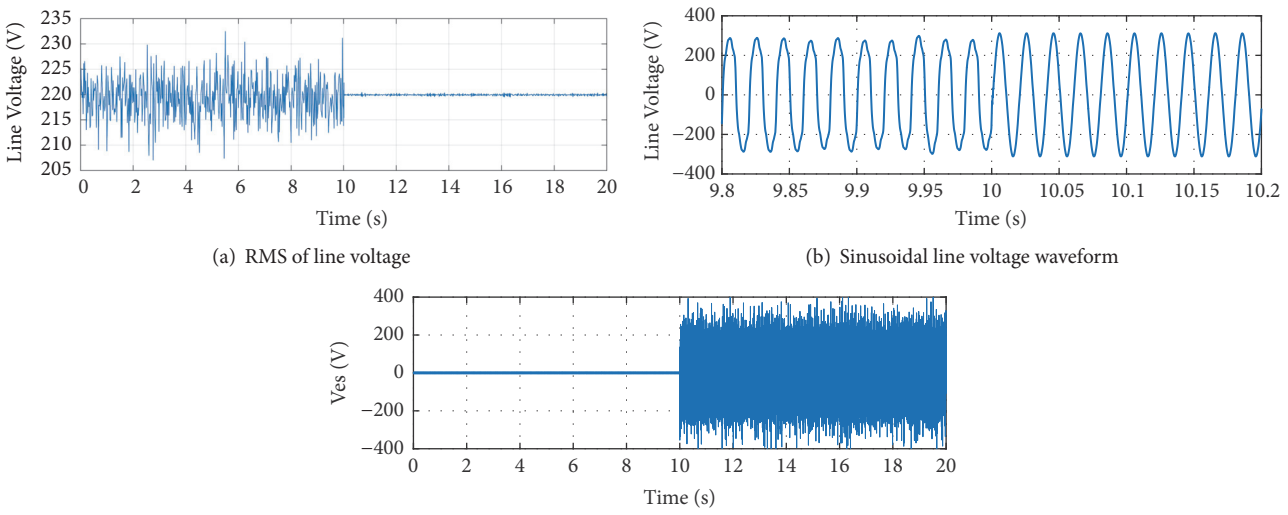

(a) RMS of line voltage

(b) Sinusoidal line voltage waveform

(c) RMS of ES voltage

Figure 7: ES regulates the line voltage under the condition of the supply voltage varying randomly. (a) RMS of line voltage, (b) sinusoidal line voltage waveform, and (c) RMS of ES voltage.

Data Availability

All data can be accessed in the Simulation Studies section of this article.

Conflicts of Interest

The authors declare that there are no conflicts of interest regarding the publication of this article.

Acknowledgments

This research was supported by the National Natural Science Foundation of China [grant number 61873129].

References

[1] J. C. Xiao, J. F. Cai, and X. D. Wang, "A hesitant fuzzy linguistic multicriteria decision-making method with interactive criteria

and its application to renewable energy projects selection," *Mathematical Problems in Engineering*, vol. 2017, Article ID 9634725, 15 pages, 2017.

[2] M. Pedrasa, T. Spooner, and I. MacGill, "Scheduling of demand side resources using binary particle swarm optimization," *IEEE Transactions on Power Systems*, vol. 24, no. 3, pp. 1173–1181, 2009.

[3] P. Palensky and D. Dietrich, "Demand side management: demand response, intelligent energy systems, and smart loads," *IEEE Transactions on Industrial Informatics*, vol. 7, no. 3, pp. 381–388, 2011.

[4] H. Cai, J. Xiang, M. Z. Q. Chen, and W. Wei, "A decentralized control strategy for photovoltaic sources to unify MPPT and DC-bus voltage regulation," in *Proceedings of the American Control Conference (ACC '17)*, pp. 2066–2071, Seattle, Wash, USA, 2017.

[5] H. Cai, J. Xiang, W. Wei, and M. Z. Chen, "V-dp/dv droop control for PV sources in DC microgrids," *IEEE Transactions on Power Electronics*, vol. 33, no. 9, pp. 7708–7720, 2018.

[6] L. Xu and P. Cartwright, "Direct active and reactive power control of DFIG for wind energy generation," *IEEE Transactions on Energy Conversion*, vol. 21, no. 3, pp. 750–758, 2006.

[7] D. F. Teshome, P. F. Correia, and K. L. Lian, "Stochastic optimization for network-constrained power system scheduling problem," *Mathematical Problems in Engineering*, vol. 2015, Article ID 694619, 17 pages, 2015.

[8] O. Abedinia and N. Amjady, "Net demand prediction for power systems by a new neural network-based forecasting engine," *Complexity*, vol. 21, no. S2, pp. 296–308, 2016.

[9] L. Xi, Y. Li, Y. Huang, L. Lu, and J. Chen, "A novel automatic generation control method based on the ecological population cooperative control for the islanded smart grid," *Complexity*, vol. 2018, Article ID 2456963, 17 pages, 2018.

[10] S. Y. Hui, C. K. Lee, and F. F. Wu, "Electric springs–a new smart grid technology," *IEEE Transactions on Smart Grid*, vol. 3, no. 3, pp. 1552–1561, 2012.

[11] X. Chen, Y. Hou, S.-C. Tan, C.-K. Lee, and S. Y. R. Hui, "Mitigating voltage and frequency fluctuation in microgrids using electric springs," *IEEE Transactions on Smart Grid*, vol. 6, no. 2, pp. 508–515, 2015.

[12] N. R. Chaudhuri, C. K. Lee, B. Chaudhuri, and S. Y. R. Hui, "Dynamic modeling of electric springs," *IEEE Transactions on Smart Grid*, vol. 5, no. 5, pp. 2450–2458, 2014.

[13] S.-C. Tan, C. K. Lee, and S. Y. Hui, "General steady-state analysis and control principle of electric springs with active and reactive power compensations," *IEEE Transactions on Power Electronics*, vol. 28, no. 8, pp. 3958–3969, 2013.

[14] X. Wei, Y. Liu, Z. Zhang, and J. Wang, "Steady-state analysis of electric spring for smart grid," in *Proceedings of the 12th World Congress on Intelligent Control and Automation*, pp. 905–909, Guilin, China, 2016.

[15] C. K. Lee, B. Chaudhuri, and S. Y. Hui, "Hardware and control implementation of electric springs for stabilizing future smart grid with intermittent renewable energy sources," *IEEE Journal of Emerging and Selected Topics in Power Electronics*, vol. 1, no. 1, pp. 18–27, 2013.

[16] C. K. Lee and S. Y. R. Hui, "Reduction of energy storage requirements in future smart grid using electric springs," *IEEE Transactions on Smart Grid*, vol. 4, no. 3, pp. 1282–1288, 2013.

[17] X. Chen, Y. Hou, and S. Y. Hui, "Distributed control of multiple electric springs for voltage control in microgrid," *IEEE Transactions on Smart Grid*, vol. 8, no. 3, pp. 1552–1561, 2017.

[18] K. T. Tan, X. Y. Peng, P. L. So, Y. C. Chu, and M. Z. Q. Chen, "Centralized control for parallel operation of distributed generation inverters in microgrids," *IEEE Transactions on Smart Grid*, vol. 3, no. 4, pp. 1977–1987, 2012.

[19] P. Kanjiya and V. Khadkikar, "Enhancing power quality and stability of future smart grid with intermittent renewable energy sources using electric springs," in *Proceedings of the 2nd International Conference on Renewable Energy Research and Applications, ICRERA '13*, pp. 918–922, Madrid, Spain, 2013.

[20] Q. Wang, M. Cheng, and Y. Jiang, "Harmonics suppression for critical loads using electric springs with current-source inverters," *IEEE Journal of Emerging and Selected Topics in Power Electronics*, vol. 4, no. 4, pp. 1362–1369, 2016.

[21] Q. Wang, M. Cheng, Z. Chen, and Z. Wang, "Steady-state analysis of electric springs with a novel δ control," *IEEE Transactions on Power Electronics*, vol. 30, no. 12, pp. 7159–7169, 2015.

[22] M. S. Javaid, U. B. Irshad, A. Hussein, and M. A. Abido, "A novel fuzzy logic controller for smart load voltage regulation," in *Proceedings of the 6th International Conference on Clean Electrical Power (ICCEP '17)*, pp. 620–624, Santa Margherita Ligure, Italy, 2017.

[23] H. Zhang and Q. Hui, "Multiagent coordination optimization based model predictive control strategy with application to balanced resource allocation," in *Proceedings of the ASME Dynamic Systems and Control Conference*, San Antonio, Tex, USA, 2014.

[24] Y. Xue, D. Meng, S. Yin et al., "Vector-based model predictive hysteresis current control for asynchronous motor," *IEEE Transactions on Industrial Electronics*.

[25] K. H. Kwan, Y. S. Png, Y. C. Qui, and P. L. So, "Model predictive control of unified power quality conditioner for power quality improvement," in *Proceedings of the IEEE International Conference on Control Applications*, pp. 916–921, Singapore, 2007.

[26] H. Zhang and Q. Hui, "Kalman filter with diffusion strategies for detecting power grid false data injection attacks," in *Proceedings of the IEEE International Conference on Electro Information Technology (EIT, '17)*, pp. 254–259, Lincoln, Neb, USA, 2017.

[27] X. D. Yan, Z. Shu, and S. M. Sharkh, "Hybrid modelling and control of single-phase grid-connected NPC inverters," in *Proceedings of the Applied Power Electronics Conference and Exposition (APEC '16)*, pp. 2223–2228, Long Beach, Calif, USA, 2016.

[28] X. Yan, Z. Shu, S. M. Sharkh, and T. Chen, "Output-feedback switching control of DC-DC cuk converters using multiple sampling," in *Proceedings of the International Automatic Control Conference (CACS '15)*, pp. 1–6, Yilan, Taiwan, 2015.

[29] Y.-C. Chu and M. Z. Q. Chen, "Efficient model predictive algorithms for tracking of periodic signals," *Journal of Control Science and Engineering*, vol. 2012, Article ID 729748, 13 pages, 2012.

[30] J. Macias and A. Gomez, "Self-tuning of kalman filters for harmonic computation," *IEEE Transactions on Power Delivery*, vol. 21, no. 1, pp. 501–503, 2006.